

# Spin liquids in frustrated magnets

Leon Balents<sup>1</sup>

**Frustrated magnets are materials in which localized magnetic moments, or spins, interact through competing exchange interactions that cannot be simultaneously satisfied, giving rise to a large degeneracy of the system ground state. Under certain conditions, this can lead to the formation of fluid-like states of matter, so-called spin liquids, in which the constituent spins are highly correlated but still fluctuate strongly down to a temperature of absolute zero. The fluctuations of the spins in a spin liquid can be classical or quantum and show remarkable collective phenomena such as emergent gauge fields and fractional particle excitations. This exotic behaviour is now being uncovered in the laboratory, providing insight into the properties of spin liquids and challenges to the theoretical description of these materials.**

Sometimes, a little frustration can make life interesting. This is true in physics, where frustration often leads to exotic properties of materials. In physics, frustration refers to the presence of competing forces that cannot be simultaneously satisfied. The concept has been applied broadly, from magnetism, which I discuss here, to negative thermal expansion of solids<sup>1</sup> and to soft materials<sup>2</sup>. Studies of frustration began with antiferromagnets, in which frustration usually has a simple geometric origin. Such geometric frustration occurs in systems of spins on lattices that involve triangular motifs (Fig. 1), in which the nearest-neighbour interactions favour anti-aligned spins (Box 1). On a triangle, the three spins cannot all be antiparallel. Instead, depending on the circumstances, the spins fluctuate, or order, in a less obvious manner.

An antiferromagnet consisting of a two-dimensional (2D) triangular lattice of Ising spins (which point either upward or downward along a single axis) provided one of the prototypes of frustration. Wannier showed in 1950 that this model has a very large degeneracy of ground states<sup>3</sup>. Now, such degeneracy is considered to be a key, or even defining, characteristic of frustration. In the triangular Ising antiferromagnet, the ground-state entropy is extensive and equals  $0.323k_B N$ , where  $k_B$  is the Boltzmann constant and  $N$  is the number of spins. At low temperatures, the spins continue to fluctuate thermally, although in a correlated manner because they are restricted to the ground states of the Ising antiferromagnet. By analogy to an ordinary liquid, in which the molecules form a dense, highly correlated state that has no static order, the spins in the triangular Ising antiferromagnet form a 'spin liquid', or cooperative paramagnet. The 'frustration' (or 'fluctuation') parameter,  $f$  (Box 1), provides a quantitative measure of the depth of the spin-liquid regime;  $f = \infty$  if the spins remain liquid down to a temperature,  $T$ , of absolute zero.

Fluctuations of the spins in a spin liquid can be classical or quantum. In quantum mechanics, the magnitude of a spin is quantized in half-integer units of  $\hbar$  (where  $\hbar$  denotes Planck's constant divided by  $2\pi$ ), the quantum of angular momentum. Classical fluctuations dominate for large spins (those with a size,  $S$ , much larger than the minimum size of  $1/2$ ) and are driven by thermal energy. Spins can be thought of as reorienting randomly with time, cycling through different microstates. When the energy  $k_B T$  becomes too small, classical fluctuations cease and the spins either freeze or order. For small spins, with  $S$  comparable to  $1/2$ , the quantum mechanical uncertainty principle produces zero-point motions comparable to the size of the spin itself, which persist down to  $T = 0$  K. Although they are similar to thermal fluctuations in some ways, quantum fluctuations can be phase coherent. If they are strong enough,

the result is a quantum spin liquid (QSL), which is a superposition state in which the spins simultaneously point in many different directions. In a QSL, the spins are highly entangled with one another in a subtle way that involves entanglement between widely separated spins. QSLs are more elusive than their classical counterparts but offer a much greater conceptual pay-off. From theory, it is predicted that they should show extremely exotic phenomena such as hosting exotic excitations with fractional quantum numbers and artificial gauge fields. They may also be associated with exotic forms of superconductivity<sup>4</sup>. Researchers are seeking QSL states in solid-state materials known as Mott insulators (in which electrons are localized to individual atomic or molecular orbitals but maintain their spin degree of freedom) and recently in artificial frustrated lattices that have been created optically for ultracold atoms.

In this Review, I survey how the discovery of new materials and improved experimental probes, together with complementary advances in theory, have reinvigorated the study of spin liquids and frustrated magnetism in general. I begin with the best-understood example of spin ice, a classical spin liquid, whose properties are far better understood after progress made in the past year. I then turn to quantum frustrated systems. After describing their basic physics, I discuss the experimental situation and its challenges. I uncover some unexpected physics in 'failures' to find QSLs. Finally, I discuss promising directions for QSL research.

## Spin ice

To begin the survey of these developments, I start with a simple example, in which the spins can be regarded as classical: spin-ice materials<sup>5,6</sup>, which were first studied by Harris and colleagues in 1997 (ref. 7). In spin ices — for example  $\text{Dy}_2\text{Ti}_2\text{O}_7$ ,  $\text{Ho}_2\text{Ti}_2\text{O}_7$  and  $\text{Ho}_2\text{Sn}_2\text{O}_7$  — only the ions of the rare-earth atoms (Dy and Ho) are magnetic, and these reside on a pyrochlore lattice, which is a network of corner-sharing tetrahedra (Fig. 1c). Their  $f$ -electron spins are large and classical, and they behave as Ising doublets aligned with the local  $\langle 111 \rangle$  axis, which connects the centres of the two tetrahedra shared by that spin. Their interactions are predominantly long range and dipolar, but much of their physics can be understood solely from an effective nearest-neighbour exchange energy,  $J_{\text{eff}}$ , which is ferromagnetic<sup>8,9</sup> (Box 2). This ferromagnetic interaction is frustrated, owing to the different Ising axes of the spins. Indeed, the states that minimize the energy of a single tetrahedron are highly degenerate, consisting of all six configurations in which two spins point inward and two spins point outward from the centre of the tetrahedron (Fig. 2a). The name spin ice originates from a direct analogy between

<sup>1</sup>Kavli Institute for Theoretical Physics, University of California, Santa Barbara, Santa Barbara, California 93106, USA.

these configurations and the positions of protons in the tetrahedrally coordinated  $O^{2-}$  framework of water ice<sup>10</sup>.

When  $k_B T \ll J_{\text{eff}}$ , the system fluctuates almost entirely within the two-in and two-out manifold of states. It turns out that the number of such states is exponentially large, so a low-temperature entropy remains even within this limit. This entropy, first estimated by Pauling in 1935 (ref. 11), has been measured in spin ice<sup>10</sup>. Although the spins remain paramagnetic in this regime, the 'ice rules' imply strong correlations: for instance, if it is known that two spins on a tetrahedron are pointing out, then the other two spins must point in. The correlated paramagnet is a simple example of a classical spin liquid. A key question is whether the local constraints have long-range consequences: is the spin liquid qualitatively distinguishable from an ordinary paramagnet? Interestingly, the answer for spin ice is 'yes'.

### Analogy to electromagnetism

To understand how long-range effects arise from a local constraint, it is helpful to use an analogy to electromagnetism. Each spin can be thought of as an arrow pointing between the centres of two tetrahedra (Fig. 2b). This defines a vector field of flux lines on the lattice, which

because of the two-in, two-out rule is divergence free. In this sense, the vectors define an 'artificial' magnetic field,  $\mathbf{b}$ , on the lattice (the field can be taken to have unit magnitude on each link, with the sign determined by the arrows). Because the spins are not ordered but fluctuating, the magnetic field also fluctuates. However, because the magnetic field lines do not start or end, these fluctuations include long loops of flux (Fig. 2b) that communicate spin correlations over long distances.

The nature of the long-distance spin correlations was derived by Youngblood and colleagues in a mathematically analogous model of a fluctuating ferroelectric, in which the electric polarization is similarly divergenceless<sup>12</sup>; this was subsequently rederived for spin ice<sup>13</sup>. The result is that the artificial magnetic field, at long wavelengths, fluctuates in equilibrium just as a real magnetic field would in a vacuum, albeit with an effective magnetic permeability. For the spins in spin ice, this implies power-law 'dipolar' correlations that are anisotropic in spin space and decay as a power law ( $\propto 1/r^3$ , where  $r$  is the distance between the spins) in real space. It is remarkable to have power-law correlations without any broken symmetry and away from a critical point. After Fourier transformation of these correlations on the lattice, a static spin structure factor with 'pinch points' at reciprocal lattice vectors in momentum space is obtained<sup>12–14</sup>.

Such dipolar correlations have recently been observed in high resolution neutron-scattering experiments by Fennell and colleagues<sup>15</sup>. At the pinch points, if the ice rules are obeyed perfectly, a sharp singularity is expected, as well as a precise vanishing of the scattering intensity along lines passing through the reciprocal lattice vectors. The rounding of this singularity gives a measure of the 'spin-ice correlation length', which is estimated to grow to 2–300 Å (a large number) at a temperature of 1.3 K. In the future, it may be interesting to see how this structure changes at even lower temperatures, at which spin ices are known to freeze and fall out of equilibrium. Although the argument of Youngblood and colleagues<sup>12</sup> and the model outlined above rely on equilibrium, arguments by Henley suggest that the pinch points could persist even in a randomly frozen glassy state<sup>14</sup>.

### Magnetic monopoles

Interestingly, the magnetostatic analogy goes beyond the equilibrium spin correlations. One of the most exciting recent developments in this area has been the discovery of magnetic monopoles in spin ice<sup>16</sup>. These arise for simple microscopic reasons. Even when  $k_B T \ll J_{\text{eff}}$ , violations of the two-in, two-out rule occur, although they are costly in energy and, hence, rare. The simplest such defect consists of a single tetrahedron with three spins pointing in and one pointing out, or vice versa (Fig. 2c). This requires an energy of  $2J_{\text{eff}}$  relative to the ground states. From a magnetic viewpoint, the centre of this tetrahedron becomes a source or sink for flux, that is, a magnetic monopole. A monopole is a somewhat non-local object: to create a monopole, a semi-infinite 'string' of spins must be flipped, starting from the tetrahedron in question (Fig. 2c). Nevertheless, when it has been created, the monopole can move by single spin flips without energy cost, at least when only the dominant nearest-neighbour exchange,  $J_{\text{eff}}$ , is considered.

Remarkably, the name monopole is physically apt: this defect carries a real 'magnetic charge'<sup>16</sup>. This is readily seen because the physical magnetic moment of the rare-earth atom is proportional to the pseudo-magnetic field,  $\mathbf{M} = g\mu_B \mathbf{b}$ , where  $g$  is the Landé  $g$  factor and  $\mu_B$  is the Bohr magneton. Thus, a monopole with the non-zero divergence  $\nabla \cdot \mathbf{b}$  also has a non-zero  $\nabla \cdot \mathbf{M}$ . The actual magnetic charge (which measures the strength of the Coulomb interaction between two monopoles) is, however, small: at the same distance, the magnetostatic force between two monopoles is approximately 14,000 times weaker than the electrostatic force between two electrons. Nevertheless, at low temperatures, this is still a measurable effect.

A flood of recent papers have identified clear signatures of magnetic monopoles in new experiments and in previously published data. Jaubert and Holdsworth showed that the energy of a monopole can be extracted from the Arrhenius behaviour of the magnetic relaxation rate<sup>17</sup>. They found that in  $Dy_2Ti_2O_7$ , the energy of a monopole is half that of a single spin flip, reflecting the fractional character of the magnetic monopoles.

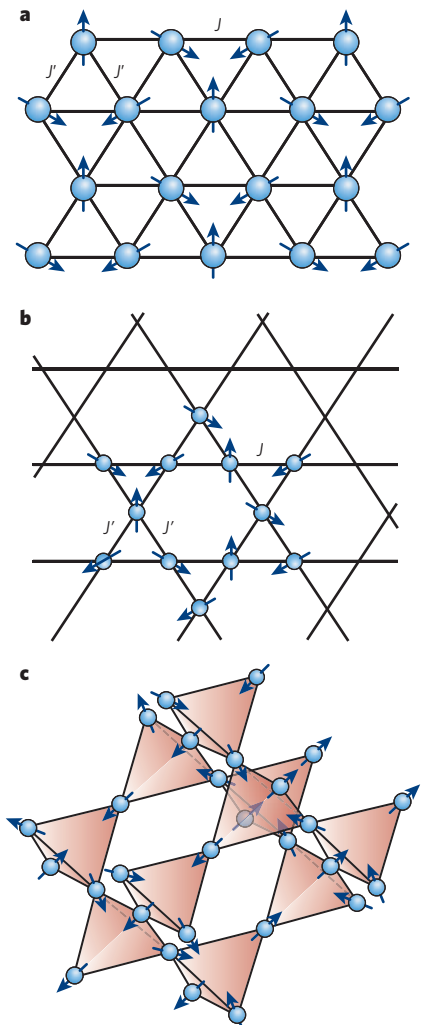


**Figure 1 | Frustrated magnetism on 2D and 3D lattices.** Two types of 2D lattice are depicted: a triangular lattice (a) and a kagomé lattice (b). The 3D lattice depicted is a pyrochlore lattice (c). In experimental materials, the three-fold rotational symmetry of the triangular and kagomé lattices may not be perfect, allowing different exchange interactions,  $J$  and  $J'$ , on the horizontal and diagonal bonds, as shown. Blue circles denote magnetic ions, arrows indicate the direction of spin and black lines indicate the shape of the lattice. In b, ions and spins are depicted on only part of the illustrated lattice.

They also identified deviations from the Arrhenius form at lower temperatures as a result of Coulomb interactions between monopoles. In an intriguing paper, Bramwell and colleagues applied an old theory put forward by Onsager<sup>18</sup> for the electric-field dependence of thermal charge dissociation in electrolytes — the Wien effect — to the magnetic analogue in spin ice, that is, to the disassociation of monopole–antimonopole pairs with a magnetic field<sup>19</sup>. The theory allows an extraction of the absolute value of the magnetic charge of a monopole from the dependence of the magnetic relaxation rate on the magnetic field. The authors measured muon spin relaxation in  $\text{Dy}_2\text{Ti}_2\text{O}_7$  to obtain the rate, and from this they extracted a magnetic charge in near perfect agreement with theoretical expectations. In addition to these quantitative measures of the energy and charge of a monopole, two recent papers presented neutron-scattering measurements in magnetic fields, interpreting them as evidence of monopoles and the ‘strings’ emanating from monopoles<sup>20,21</sup>. Many more experiments in which the monopoles in spin ice are studied and manipulated are likely to emerge soon.

### Quantum spin liquids

In spin ice, as the temperature is lowered, the spins themselves fluctuate ever more slowly, eventually falling out of equilibrium and freezing below about 0.5 K (from theory, it is predicted that, in equilibrium, the spins should order at  $T=0.1\text{--}0.2$  K (ref. 6)). This is a consequence of the large energy barriers between different ice-rule configurations, which require the flipping of at least six spins, and the weak quantum amplitude for such large spins to cooperatively tunnel through these barriers. By contrast, for materials with spins of  $S=\frac{1}{2}$  and approximate Heisenberg symmetry, quantum effects are strong, and there are no obvious energy barriers. I now turn to such materials in the search for a QSL ground state, in which spins continue to fluctuate and evade order even at  $T=0$  K. Such a QSL is a strange beast: it has a non-magnetic ground state that is built from well-formed local moments. The theoretical possibility of QSLs has been hotly debated since Anderson proposed them in 1973 (ref. 22).

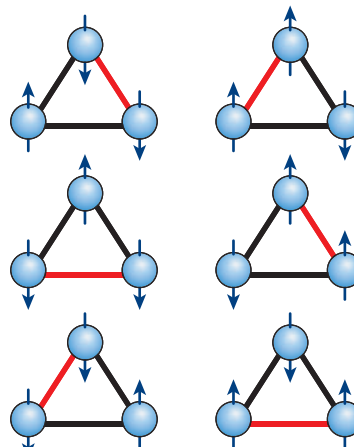
### Wavefunctions and exotic excitations

A natural building block for non-magnetic states is the valence bond, a pair of spins that, owing to an antiferromagnetic interaction, forms a spin-0 singlet state (Fig. 3a). A valence bond is a highly quantum object, the two spins being maximally entangled and non-classical. If all of the spins in a system are part of valence bonds, then the full ground state has spin 0 and is non-magnetic. One way in which this can occur is by the partitioning of all of the spins into specific valence bonds, which are static and localized. Mathematically, such a ground state is well approximated as a product of the valence bonds, so that each spin is highly entangled with only one other, its valence-bond partner. This is known as a valence-bond solid (VBS) state (Fig. 3a) and occurs in several materials<sup>23–25</sup>. VBS states are interesting because, for instance, they provide an experimental way of studying Bose–Einstein condensation of magnons (which are triplet excitations of the singlet valence bonds) in the solid state<sup>26</sup>.

A VBS state is not, however, a true QSL, because it typically breaks lattice symmetries (because the arrangement of valence bonds is not unique) and lacks long-range entanglement. To build a QSL, the valence bonds must be allowed to undergo quantum mechanical fluctuations. The ground state is then a superposition of different partitionings of spins into valence bonds (Fig. 3b, c). If the distribution of these partitionings is broad, then there is no preference for any specific valence bond and the state can be regarded as a valence-bond ‘liquid’ rather than a solid. This type of wavefunction is generally called a resonating valence-bond (RVB) state<sup>22</sup>. RVB states became subjects of intense theoretical interest when, in 1987, Anderson proposed that they might underlie the physics of high-temperature superconductivity<sup>4</sup>. Only relatively recently, however, have RVB wavefunctions been shown to be ground states of many specific model Hamiltonians<sup>27–32</sup>.

It is now understood that not all QSLs are alike. Generally, different states have different weights of each valence-bond partition in their wavefunctions. The valence bonds need not be formed only from nearby

### Box 1 | Elements of frustration



A triangle of antiferromagnetically interacting Ising spins, which must point upward or downward, is the simplest example of frustration. All three spins cannot be antiparallel. As a result, instead of the two ground states mandated by the Ising symmetry (up and down), there are six ground states (see figure; blue circles denote magnetic ions, arrows indicate the direction of spin, and black and red lines indicate the shape of the triangular lattice, with red lines denoting the axis on which the spins are parallel). On 2D and 3D lattices, such degeneracies can persist. When they do, fluctuations are enhanced and ordering is suppressed. On the basis of this fact, Ramirez introduced a simple empirical measure of frustration that has become widely used<sup>50</sup>. At high temperatures, the spin (or magnetic) susceptibility of a local-moment magnet generally has a Curie–Weiss form,  $\chi \approx C/(T - \Theta_{\text{CW}})$ , where  $T$  is temperature and  $C$  is the Curie constant. This allows extraction of the Curie–Weiss temperature,  $\Theta_{\text{CW}}$ , from a plot of  $1/\chi$  versus  $T$ .  $|\Theta_{\text{CW}}|$  provides a natural estimate for the strength of magnetic interactions ( $\Theta_{\text{CW}} < 0$  for an antiferromagnet) and sets the scale for magnetic ordering in an unfrustrated material. By comparing the Curie–Weiss temperature with the temperature at which order freezes,  $T_c$ , the frustration parameter,  $f$ , is obtained:  $f = |\Theta_{\text{CW}}|/T_c$ . Typically,  $f > 5\text{--}10$  indicates a strong suppression of ordering, as a result of frustration. For such values of  $f$ , the temperature range  $T_c < T < |\Theta_{\text{CW}}|$  defines the spin-liquid regime.

spins<sup>33</sup>. If a valence bond is formed from spins that are far apart, then those spins are only weakly bound into a singlet and the valence bond can be ‘broken’ to form free spins with relatively little energy. So states that have a significant weight from long-range valence bonds have more low-energy spin excitations than states in which the valence bonds are mainly short range (see, for example, ref. 34). There are also other excitations that do not break the valence bonds but simply rearrange them. Such excitations can have low energy even in short-range RVB states.

Given the possibility of different QSL states, it is interesting to attempt to classify these states. This problem is only partly solved, but it is clear that the number of possible states is huge, if not infinite. For instance, Wen has classified hundreds of different ‘symmetrical spin liquids’ (QSLs with the full space-group symmetry) for  $S=\frac{1}{2}$  antiferromagnets on the square lattice<sup>35</sup>. Finding the correct QSL ground state among all of the many possible RVB phases, many of which have similar energies, is a challenge to theory, reminiscent of the landscape problem in string theory, in high-energy physics.

Even with this diversity of possible states, one feature that theorists expect QSLs to have in common is that they support exotic excitations. What is meant by exotic? In most phases of matter, all of the excitations can be constructed from elementary excitations that are either electron-like (spin  $S=\frac{1}{2}$  and charge  $\pm e$ ) or magnon-like (spin  $S=1$  and charge neutral). Only in rare examples, such as the fractional quantum Hall states, do the elementary excitations differ from these, in this case by carrying fractional quantum numbers. The magnetic monopoles in spin

**Box 2 | Theoretical frameworks**

Theoretical models of magnets with localized electrons typically start with the Heisenberg Hamiltonian, for example:

$$H = -\frac{1}{2} \sum_{ij} J_{ij} \mathbf{S}_i \cdot \mathbf{S}_j \quad (1)$$

where  $J_{ij}$  are exchange constants, and  $\mathbf{S}_i$  and  $\mathbf{S}_j$  are quantum spin- $S$  operators. They obey  $S_i^2 = S(S+1)$  and canonical commutation relations  $[S_i^\mu, S_j^\nu] = i\epsilon_{\mu\nu\lambda} S_i^\lambda \delta_{ij}$ , where  $\epsilon_{\mu\nu\lambda}$  is the Levi-Civita symbol. In spin ice, owing to the large  $S$  ( $S=15/2$  for Dy and 8 for Ho), the spins can be regarded simply as classical vectors (conventionally they are taken to be of unit length, with factors of  $S$  absorbed into the exchange constants). For spin ice, equation (1) above mimics the short-range effect of dipolar exchange, by taking ferromagnetic  $J_{ij} = J_{eff} > 0$  on nearest neighbours, as is discussed in the main text. In addition, in spin ice, strong Ising anisotropy must be included by way of the crystal field term

$$H_{cf} = -D \sum_i (\mathbf{S}_i \cdot \hat{\mathbf{n}})^2$$

where  $\hat{\mathbf{n}}$  is a unit vector along the Ising  $\langle 111 \rangle$  axis of the  $i$ th spin and  $D$  is the Ising anisotropy. The positive  $D \gg J$  requires the spins to point along this axis. In low-spin systems of transition metal spins, the exchange is antiferromagnetic,  $J_{ij} < 0$ , crystal field effects are much less significant and  $S$  is much smaller. For the QSL candidates discussed in the main text,  $S$  takes its minimum value,  $1/2$ . Thus, when the assumption of localized electrons is valid, equation (1) itself is a good starting point. If this assumption is not valid, a better description, which includes charge fluctuations, is the Hubbard model:

$$H_{Hubbard} = -\sum_{ij,\alpha} t_{ij} c_{i\alpha}^\dagger c_{j\alpha} + U \sum_i n_i(n_i - 1)$$

where  $c_{i\alpha}^\dagger$  and  $c_{i\alpha}$  are creation and annihilation operators, respectively, for electrons with spin  $\alpha = \pm 1/2$  on site  $i$ , and  $n_i = \sum_\alpha c_{i\alpha}^\dagger c_{i\alpha}$  is the number of electrons on the site. The electron operators obey canonical anti-commutation relations  $\{c_{i\alpha}^\dagger, c_{j\beta}\} = \delta_{ij}\delta_{\alpha\beta}$ . The coefficient  $t_{ij}$  gives the quantum amplitude for an electron to hop from site  $j$  to site  $i$ , and  $U$  is the Coulomb energy cost for two electrons to occupy the same site. When  $U \gg t$ , and there is on average one electron per site, charge fluctuations become negligible. Then the Hubbard model reduces to the Heisenberg one, with  $J_{ij} \approx -4t_{ij}^2/U$ . However, when  $U/t$  is not very large, the two models are inequivalent. For a small enough  $U/t$ , the Hubbard model usually describes a metal, in which electrons are completely delocalized. As  $U/t$  is increased from zero, there is a quantum phase transition from a metal to an insulator; this is known as the Mott transition. For  $U/t$  larger than this critical value, the system is known as a Mott insulator. 'Weak' Mott insulators are materials with  $U/t$  close to the Mott transition.

is in equilibrium, corrections to this form would be expected to lead to monopole confinement at low temperatures.

In a true 2D or 3D QSL, the string associated with a spinon remains robustly tensionless even at  $T=0$  K, owing to strong quantum fluctuations (Fig. 4c). This can be understood from the quantum superposition principle: rearranging the spins along the string simply reshuffles the various spin or valence-bond configurations that are already superposed in the ground state. Detailed studies of QSL states have shown that higher-dimensional spinons can have varied character. They may obey Fermi-Dirac<sup>36</sup>, Bose-Einstein<sup>37</sup> or even anyonic statistics (see page 187). They may be gapped (that is, require a non-zero energy to excite) or gapless, or they may even be so strongly interacting that there are no sharp excitations of any kind<sup>38</sup>.

**Experimental search for QSLs**

In contrast to the apparent ubiquity and variety of QSLs in theory, the experimental search for QSLs has proved challenging. Most Mott insulators — materials with localized spins — are ordered magnetically or freeze into spin-glass states. A much smaller set of Mott insulators form VBS states<sup>23–25</sup>. A clear identification of RVB-like QSL states has proved more elusive.

How is a QSL identified in experiments? One good indication is a large frustration parameter,  $f > 100–1,000$  ( $f$  may be limited by material complications, such as defects or weak symmetry-breaking interactions, or the ability to cool). A more stringent test is the absence of static moments, even disordered ones, at low temperatures, a feature that can be probed by nuclear magnetic resonance (NMR) and muon spin resonance experiments. Specific-heat measurements give information on the low-energy density of states of a putative QSL, which can be compared with those of theoretical models. Thermal transport can determine whether these excitations are localized or itinerant. Elastic and inelastic neutron-scattering measurements, especially on single crystals, provide crucial information on the nature of correlations and excitations, and these could perhaps uncover spinons. All told, this is a powerful arsenal of experimental tools, but the task is extremely challenging. At the heart of the problem is that there is no single experimental feature that identifies a spin-liquid state. As long as a spin liquid is characterized by what it is not — a symmetry-broken state with conventional order — it will be much more difficult to identify conclusively in experiments.

Nevertheless, in recent years, increased activity in the field of highly frustrated magnetism has led to a marked increase in the number of candidate QSL materials, giving reason for optimism<sup>39,40</sup>. A partial list of the materials that have been studied is presented in Table 1.

**QSL materials**

The last two entries in Table 1 ( $\text{Cs}_2\text{CuCl}_4$  and  $\text{FeSc}_2\text{S}_4$ ) have already been ruled out as true QSLs, and I return to these later (in the section 'Unexpected findings'). All of the remaining materials are promising candidates, with  $S = 1/2$  quantum spins on frustrated lattices. They show persistent spin dynamics down to the lowest measured temperatures, with every indication that the dynamics persist down to  $T=0$  K. With the exception of  $\text{Cu}_3\text{V}_2\text{O}_7(\text{OH})_2 \cdot 2\text{H}_2\text{O}$ , no signs of phase transitions are seen on cooling from the high-temperature paramagnet to a low temperature. The characteristics of these materials are now beginning to be understood.

Surveying them, it is clear that there is a variety of structures and properties. There are organic compounds —  $\kappa$ -(BEDT-TTF) $2\text{Cu}_2(\text{CN})_3$  and  $\text{EtMe}_3\text{Sb}[\text{Pd}(\text{dmit})_2]_2$  — and a variety of inorganic compounds. The spins form several different structures: 2D triangular lattices; 2D kagomé lattices; and a hyperkagomé lattice, which is 3D. In some cases, these are ideal, isotropic forms. In other cases, there are asymmetries and, consequently, spatial anisotropy. Existing samples are compromised by varying degrees of disorder, from as much as 5–10% free defect spins and a similar concentration of spin vacancies in  $\text{ZnCu}_3(\text{OH})_6\text{Cl}_2$  (ref. 41) to as little as 0.07% impurity in recently improved samples of  $\text{Cu}_3\text{V}_2\text{O}_7(\text{OH})_2 \cdot 2\text{H}_2\text{O}$  (ref. 42). In several materials, the nature and degree of disorder have not been well characterized.

ice are examples of this: the elementary magnetic dipole 'splits' into a monopole–antimonopole pair. However, these are classical excitations and not true coherent quasiparticles. In QSLs, the most prominent exotic excitations are in the form of spinons, which are neutral and carry spin  $S = 1/2$  (Fig. 4). Spinons are well established in one-dimensional (1D) systems, in which they occur as domain walls (Fig. 4a). A spinon can thus be created similarly to a monopole in spin ice, by flipping a semi-infinite string of spins. A key difference, however, is that in one dimension the only boundary of such a string is its end point, so the string is guaranteed to cost only a finite energy from this boundary. By contrast, in two or three dimensions, the boundary of a string extends along its full length. A string would naturally be expected to have a tension (that is, there is an energy cost proportional to its length). String tension represents confinement of the exotic particle, as occurs for quarks in quantum chromodynamics. This is avoided in spin ice by the special form of the nearest-neighbour Hamiltonian. However, when spin ice

A key physical distinction among the candidates is their degree of charge localization — this is important for understanding the mechanism of the spin-liquid behaviour. The kagomé materials can be regarded as strong Mott insulators, in which the electrons constituting the spins are approximately localized to a single atomic orbital. This can be seen from the small exchange couplings (proportional to the Curie-Weiss temperature,  $\Theta_{\text{CW}}$ ) relative to the Mott charge gap, which is of the order of electronvolts (eV) in such copper oxides. For these materials, a microscopic description purely in terms of Heisenberg spins is justified. By contrast, for the organic compounds and  $\text{Na}_4\text{Ir}_3\text{O}_8$ , the exchange energies are larger and the charge gaps are smaller. These materials are therefore weak Mott insulators, in which the electronic spins are much less well localized, so charge fluctuations may have an important role. In the organic compounds, the Hubbard repulsion,  $U$  (Box 2), which sets the Mott gap, is much smaller than in inorganic compounds, owing to the extended nature of the molecular orbital constituting each spin. In  $\text{Na}_4\text{Ir}_3\text{O}_8$ ,  $U$  is likewise reduced because 5d orbitals are significantly larger than 3d ones. The fact that metal–insulator transitions can be induced by physical pressure or chemical pressure in all three cases (for the two organic compounds and  $\text{Na}_4\text{Ir}_3\text{O}_8$ )<sup>43,44</sup>, and the fact that in  $\kappa\text{-}(\text{BEDT-TTF})_2\text{Cu}_2(\text{CN})_3$  no clear Mott gap is seen spectroscopically<sup>45</sup>, is direct experimental evidence that these materials are weak Mott insulators. The applicability of a Heisenberg spin description to these materials is thus open to question.

Thermodynamic studies of these materials are also important because they reveal the spectrum of low-energy states, an abundance of which is expected in frustrated systems. At very low temperatures, the functional form of the specific heat and sometimes the spin (or magnetic) susceptibility can distinguish between QSLs. The general thermodynamic features of the materials are remarkably similar. In all cases in which it has been measured, the magnetic specific heat shows a peak well below the Curie–Weiss temperature<sup>46–49</sup>, indicating that significant spin entropy is maintained above this peak temperature. This specific heat then gradually decreases on further lowering of the temperature, in a manner that can roughly be fitted to a quadratic behaviour,  $C_v \approx AT^2$ , where  $C_v$  is molar specific heat at constant volume and  $A$  is a constant. This non-exponential form clearly indicates the absence of an energy gap. However, some caution is in order before interpreting this as characteristic of QSLs: such approximately quadratic behaviour of  $C_v$  is common in frustrated magnets, even ones that are classical and for which QSL physics is clearly irrelevant<sup>50</sup>. At very low temperatures, the candidate QSL materials generally show a linear behaviour,  $C_v \approx \gamma T$ , where  $\gamma$  is the Sommerfeld coefficient (refs 46–49, 51), which varies widely (between 1 and 250 mJ K<sup>-2</sup> mol<sup>-1</sup>). This is evidence of a large density of low-energy states.

Ideally, the spin susceptibility,  $\chi$ , is a useful measure of the available low-energy spin excitations. All of the candidate QSL materials also show a large Pauli-like paramagnetic susceptibility,  $\chi_0$ , in the zero-temperature limit. This susceptibility is smallest for the organic compounds: for these,  $\chi_0 \approx 3 \times 10^{-4}$  e.m.u. mol<sup>-1</sup> (refs 52, 53), whereas it is 3–10 times larger for the inorganic compounds<sup>41,42,46,47,49</sup>. Before these values of  $\chi_0$  can be interpreted as additional evidence for gapless excitations in QSLs, it is important to consider the influence of spin–orbit coupling. Spin–orbit coupling generally leads to a non-zero  $\chi_0$  value irrespective of the presence or absence of an energy gap. An empirical indicator of the importance of spin–orbit coupling is the Wilson ratio, which is defined as

$$R = \frac{4\pi^2 k_B^2 \chi_0}{3(g\mu_B)^2 \gamma} \quad (1)$$

and should be, at most, of order 1 in the absence of strong ferromagnetic tendencies or spin–orbit coupling. Because all of the candidate QSL materials are strongly antiferromagnetic, the ferromagnetic interpretation is untenable. In fact, most (but not all) QSL theories, in the absence of spin–orbit coupling, predict that  $R \ll 1$ . By contrast, the measured Wilson ratios for all of the QSL candidates in Table 1 are significantly

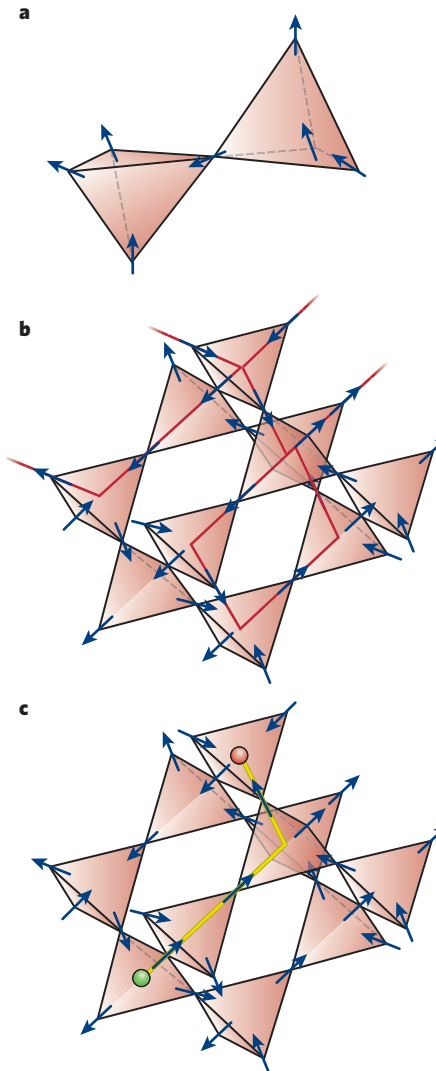


**Figure 2 | Spins, artificial magnetic fields and monopoles in spin ice.** **a**, A ground-state configuration of spins is shown in a pyrochlore lattice. The spins obey the constraint of the ice rules that mandates two inward-pointing spins and two outward-pointing ones on each tetrahedron. **b**, For the same lattice type, some of the loops of ‘magnetic flux’ are shown (red lines), as defined by the mapping of spins to an artificial magnetic field. **c**, For the same lattice type, a monopole (green) and antimonopole (red) are shown. These are created by flipping the ‘string’ of spins connected by the yellow line (compare with the spins in **b**). For simplicity, the particles themselves are not depicted. Note that the spins on the tetrahedron containing a monopole (antimonopole) orient three-in, one-out (three-out, one-in), violating the ice rules.

larger than 1, with the exception of  $\text{ZnCu}_3(\text{OH})_6\text{Cl}_2$  (for which an estimate of the intrinsic  $\gamma$  value, uncontaminated by impurities, is not available) and  $\kappa\text{-}(\text{BEDT-TTF})_2\text{Cu}_2(\text{CN})_3$ . The value of the Wilson ratio for  $\text{ZnCu}_3(\text{OH})_6\text{Cl}_2$  is probably suppressed by the high degree of disorder. The extremely large value for  $\text{Na}_4\text{Ir}_3\text{O}_8$  ( $R = 70$ ) indicates very strong spin–orbit effects, which are not surprising given the large atomic number of iridium.

The most direct evidence for a lack of magnetic ordering comes from local probe measurements, by using techniques such as NMR and muon spin resonance, in which local fields resulting from static moments affect the nuclear or muon spins and can be readily detected by their influence on the muon spins. Such measurements have confirmed the absence of local static moments down to  $T = 32$  mK in  $\kappa\text{-}(\text{BEDT-TTF})_2\text{Cu}_2(\text{CN})_3$  (ref. 52),  $T = 1.37$  K in  $\text{EtMe}_3\text{Sb}[\text{Pd}(\text{dmit})_2]_2$  (ref. 54) and  $T = 50$  mK in  $\text{ZnCu}_3(\text{OH})_6\text{Cl}_2$  (ref. 55). However, in  $\text{Cu}_3\text{V}_2\text{O}_7(\text{OH})_2 \cdot 2\text{H}_2\text{O}$ , magnetic

order and/or freezing is observed, by using NMR spectroscopy, at  $T < 1$  K (ref. 56). Moreover, recent experiments show that this compound has a complex series of low-temperature phases in an applied magnetic field<sup>56</sup>. Given the exceptionally high purity of  $\text{Cu}_3\text{V}_2\text{O}_7(\text{OH})_2 \bullet 2\text{H}_2\text{O}$ , an explanation of its phase diagram should be a clear theoretical goal.

### Theoretical interpretations

I now turn to the theoretical evidence for QSLs in these systems and how the experiments can be reconciled with theory. Theorists have attempted to construct microscopic models for these materials (Box 2) and to determine whether they support QSL ground states. In the case of the organic compounds, these are Hubbard models, which account for significant charge fluctuations. For the kagomé materials, a Heisenberg model description is probably appropriate. There is general theoretical agreement that the Hubbard model for a triangular lattice has a QSL ground state for intermediate-strength Hubbard repulsion near the Mott transition<sup>57–59</sup>. On the kagomé lattice, the Heisenberg model is expected to have a non-magnetic ground state as a result of frustration<sup>60</sup>. Recently, there has been growing theoretical support for the conjecture that the ground state is, however, not a QSL but a VBS with a large, 36-site, unit cell<sup>61,62</sup>. However, all approaches indicate that many competing states exist, and these states have extremely small energy differences from this VBS state. Thus, the ‘real’ ground state in the kagomé materials is probably strongly perturbed by spin-orbit coupling, disorder, further-neighbour interactions and so on<sup>63</sup>. A similar situation applies to the hyperkagomé lattice of  $\text{Na}_4\text{Ir}_3\text{O}_8$  (ref. 64).

These models are difficult to connect directly, and in detail, to experiments, which mainly measure low-energy properties at low temperatures. Instead, attempts to reconcile theory and experiment in detail have relied on more phenomenological low-energy effective theories of QSLs. Such effective theories are similar in spirit to the Fermi liquid theory of interacting metals: they propose that the ground state has a certain structure and a set of elementary excitations that are consistent with this structure. In contrast to the Fermi liquid case, however, the elementary excitations consist of spinons and other exotic particles, which are coupled by gauge fields. A theory of this type — that is, proposing a ‘spinon Fermi surface’ coupled to a U(1) gauge field — has had some success in explaining data from experiments on  $\kappa$ -(BEDT-TTF)<sub>2</sub> $\text{Cu}_2(\text{CN})_3$  (refs 65, 66). Related theories have been proposed for  $\text{ZnCu}_3(\text{OH})_6\text{Cl}_2$  (ref. 67) and  $\text{Na}_4\text{Ir}_3\text{O}_8$  (ref. 68). However, comparisons

for these materials are much more limited. In all cases, the comparison of theory with experiment has, so far, been indirect. I return to this problem in the subsection ‘The smoking gun for QSLs’.

### Unexpected findings

In the course of a search as difficult as the one for QSLs, it is natural for there to be false starts. In several cases, researchers uncovered other interesting physical phenomena in quantum magnetism.

### Dimensional reduction in $\text{Cs}_2\text{CuCl}_4$

$\text{Cs}_2\text{CuCl}_4$  is a spin- $1/2$  antiferromagnet on a moderately anisotropic triangular lattice<sup>69,70</sup>. It shows only intermediate frustration, with  $f \approx 8$ , ordering into a spiral Néel state at  $T_N = 0.6$  K. However, neutron-scattering results for this compound reported by Coldea and colleagues suggested that exotic physical phenomena were occurring<sup>69,70</sup>. These experiments measure the type of excitation that is created when a neutron interacts with a solid and flips an electron spin. In normal magnets, this creates a magnon and, correspondingly, a sharp resonance is observed when the energy and momentum transfer of the neutron equal that of the magnon. In  $\text{Cs}_2\text{CuCl}_4$ , this resonance is extremely small. Instead, a broad scattering feature is mostly observed. The interpretation of this result is that the neutron’s spin flip creates a pair of spinons, which divide the neutron’s energy and momentum between them. The spinons were suggested to arise from an underlying 2D QSL state.

A nagging doubt with respect to this picture was the striking similarity between some of the spectra in the experiment and those of a 1D spin chain, in which 1D spinons indeed exist<sup>71</sup>. In fact, in  $\text{Cs}_2\text{CuCl}_4$  the exchange energy along one ‘chain’ direction is three times greater than along the diagonal bonds between chains (that is,  $J' \approx J/3$  in Fig. 1a). Experimentally, however, the presence of substantial transverse dispersion (that is, dependence of the neutron peak on momentum perpendicular to the chain axis in  $\text{Cs}_2\text{CuCl}_4$ ), and the strong influence of interchain coupling on the magnetization curve,  $M(H)$ , seemed to rule out a 1D origin, despite an early theoretical suggestion<sup>72</sup>.

In the past few years, it has become clear that discarding the idea of 1D physics was premature<sup>73,74</sup>. It turns out that although the interchain coupling is substantial, and thus affects the  $M(H)$  curve significantly, the frustration markedly reduces interchain correlations in the ground state. As a result, the elementary excitations of the system are similar to those of 1D chains, with one important exception. Because the

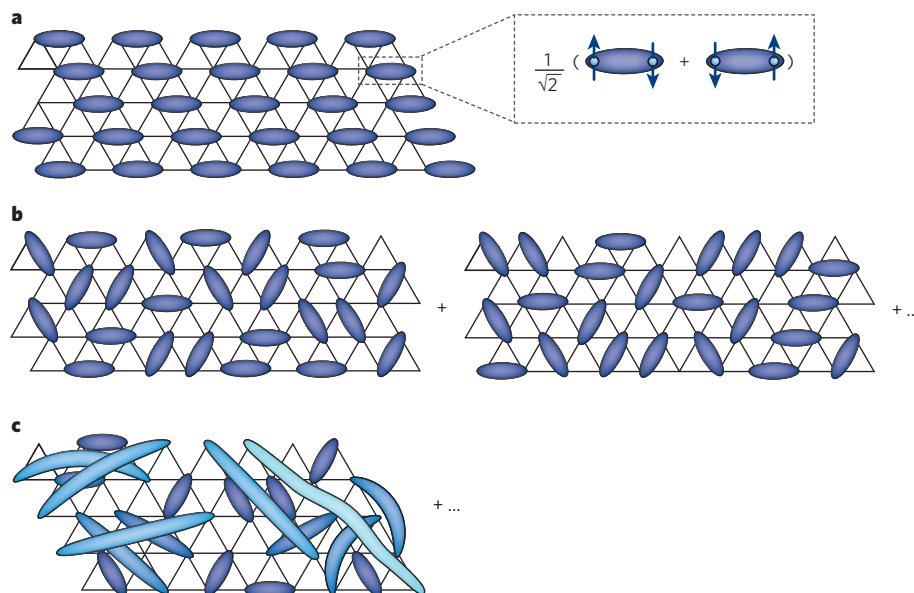


**Figure 3 | Valence-bond states of frustrated antiferromagnets.** In a VBS state (a), a specific pattern of entangled pairs of spins — the valence bonds — is formed. Entangled pairs are indicated by ovals that cover two points on the triangular lattice. By contrast, in a RVB state, the wavefunction is a

superposition of many different pairings of spins. The valence bonds may be short range (b) or long range (c). Spins in longer-range valence bonds (the longer, the lighter the colour) are less tightly bound and are therefore more easily excited into a state with non-zero spin.

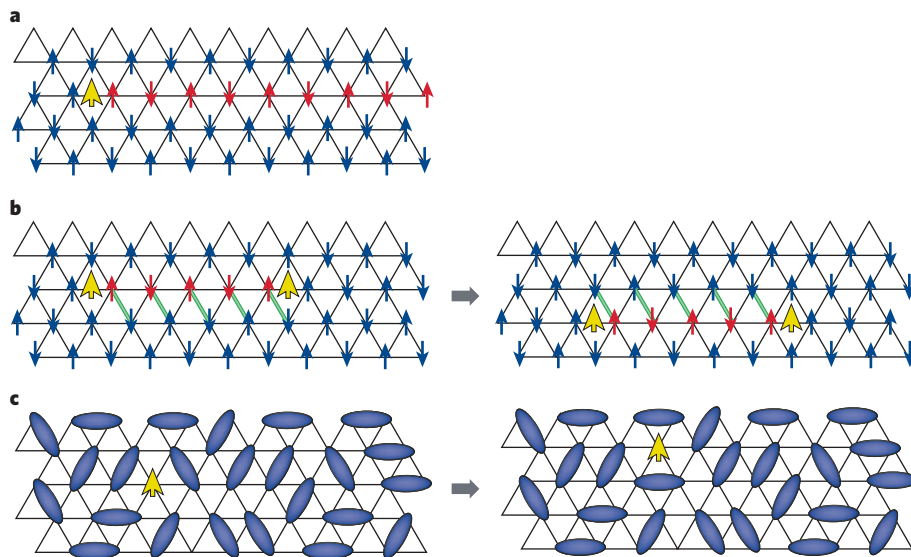


**Figure 4 | Excitations of quantum antiferromagnets.** **a**, In a quasi-1D system (such as the triangular lattice depicted), 1D spinons are formed as a domain wall between the two antiferromagnetic ground states. Creating a spinon (yellow arrow) thus requires the flipping of a semi-infinite line of spins along a chain, shown in red. The spinon cannot hop between chains, because to do so would require the coherent flipping of an infinite

number of spins, in this case all of the red spins and their counterparts on the next chain. **b**, A bound pair of 1D spinons forms a triplon. Because a finite number of spins are flipped between the two domain walls (shown in red), the triplon can coherently move between chains, by the flipping of spins along the green bonds. **c**, In a 2D QSL, a spinon is created simply as an unpaired spin, which can then move by locally adjusting the valence bonds.

spinons are inherently 1D, they are confined to the chains, and to take advantage of the transverse exchange, they must be bound into  $S=1$  ‘triplon’ bound states (Fig. 3b). These triplons move readily between chains and are responsible for the transverse dispersion observed in the experiment. Thus, the observation of triplons provides a means to distinguish 1D spinons from their higher-dimensional counterparts. A quantitative theory of this physics agrees well with the data, with no adjustable parameters. It is therefore understood that  $\text{Cs}_2\text{CuCl}_4$  is an example of ‘dimensional reduction’ induced by frustration and quantum fluctuations. This phenomenon was unexpected and might have a role in other correlated materials. Perhaps it is related to the cascade of phases that is observed in the isostructural material  $\text{Cs}_2\text{CuBr}_4$  in applied magnetic fields<sup>75</sup>.

#### Spin-orbital quantum criticality in $\text{FeSc}_2\text{S}_4$

Among the entries in Table 1,  $\text{FeSc}_2\text{S}_4$  stands out as a material that has not only spin degeneracy but also orbital degeneracy. This is common in transition-metal-containing compounds<sup>76,77</sup>. It is possible to imagine a quantum orbital liquid<sup>78–80</sup>, analogous to a QSL. Like the more familiar (theoretically) QSL, the quantum orbital liquid is experimentally elusive. Nevertheless, experimentalists have observed that  $\text{FeSc}_2\text{S}_4$ , which has a twofold orbital degeneracy, evades order down to  $T=50\text{ mK}$ , and on this basis it was characterized as a spin-orbital liquid<sup>81–83</sup>.

Recently, it was suggested that this liquid behaviour is due not to frus-

tration but to a competition between spin-orbit coupling and magnetic exchange<sup>84</sup>. Microscopic estimates of the spin-orbit interaction,  $\lambda$ , indeed show that its strength,  $\lambda/k_B=25–50\text{ K}$ , is comparable to the Curie-Weiss temperature, 45 K. As a result, the material is serendipitously close to a quantum critical point between a magnetically ordered state and a ‘spin-orbital singlet’, induced by spin-orbit coupling<sup>84</sup> (Fig. 5). This picture seems to explain data from a variety of experiments, including NMR<sup>81</sup>, neutron-scattering<sup>82</sup>, spin susceptibility<sup>83</sup> and specific-heat<sup>83</sup> measurements. Most notably, the anomalously small excitation gap of 2 K that was measured in neutron-scattering<sup>82</sup> and NMR<sup>81</sup> experiments is understandable — this gap vanishes on approaching the quantum critical point. If the theory is correct,  $\text{FeSc}_2\text{S}_4$  can be viewed as a kind of spin-orbital liquid with significant long-distance entanglement between spins and orbitals. Because the material is not precisely at the quantum critical point, however, there is a finite correlation length; therefore, this entanglement does not persist to arbitrarily long distances, as would be expected in a true RVB state.

#### Future directions

I have only touched the surface of the deep well of phenomena to be explored, experimentally and theoretically, in frustrated magnets and spin liquids. In spin ice, there are subtle correlations, collective excitations and emergent magnetic monopoles, all of which are highly amenable to laboratory studies. In several frustrated magnets with spin

**Table 1 | Some experimental materials studied in the search for QSLs**

Material	Lattice	$S$	$\Theta_{\text{CW}}$ (K)	$R^*$	Status or explanation
$\kappa$ -(BEDT-TTF) <sub>2</sub> $\text{Cu}_2(\text{CN})_3$	Triangular <sup>†</sup>	$\frac{1}{2}$	-375 <sup>‡</sup>	1.8	Possible QSL
$\text{EtMe}_5\text{Sb}[\text{Pd}(\text{dmft})_2]_2$	Triangular <sup>†</sup>	$\frac{1}{2}$	-(375–325) <sup>‡</sup>	?	Possible QSL
$\text{Cu}_3\text{V}_2\text{O}_7(\text{OH})_2 \bullet 2\text{H}_2\text{O}$ (volborthite)	Kagomé <sup>†</sup>	$\frac{1}{2}$	-115	6	Magnetic
$\text{ZnCu}_3(\text{OH})_6\text{Cl}_2$ (herbertsmithite)	Kagomé	$\frac{1}{2}$	-241	?	Possible QSL
$\text{BaCu}_3\text{V}_2\text{O}_8(\text{OH})_2$ (vesignieite)	Kagomé <sup>†</sup>	$\frac{1}{2}$	-77	4	Possible QSL
$\text{Na}_4\text{Ir}_3\text{O}_8$	Hyperkagomé	$\frac{1}{2}$	-650	70	Possible QSL
$\text{Cs}_2\text{CuCl}_4$	Triangular <sup>†</sup>	$\frac{1}{2}$	-4	0	Dimensional reduction
$\text{FeSc}_2\text{S}_4$	Diamond	2	-45	230	Quantum criticality

<sup>†</sup>BEDT-TTF, bis(ethylenedithio)-tetraphiafulvalene; dmft, 1,3-dithiole-2-thione-4,5-dithiolate; Et, ethyl; Me, methyl. <sup>\*</sup> $R$  is the Wilson ratio, which is defined in equation (1) in the main text. For  $\text{EtMe}_5\text{Sb}[\text{Pd}(\text{dmft})_2]_2$  and  $\text{ZnCu}_3(\text{OH})_6\text{Cl}_2$ , experimental data for the intrinsic low-temperature specific heat are not available, hence  $R$  is not determined. <sup>†</sup>Some degree of spatial anisotropy is present, implying that  $J \neq J$  in Fig. 1a. <sup>‡</sup>A theoretical Curie-Weiss temperature ( $\Theta_{\text{CW}}$ ) calculated from the high-temperature expansion for an  $S = \frac{1}{2}$  triangular lattice;  $\Theta_{\text{CW}} = 3J/2k_B$ , using the  $J$  fitted to experiment.

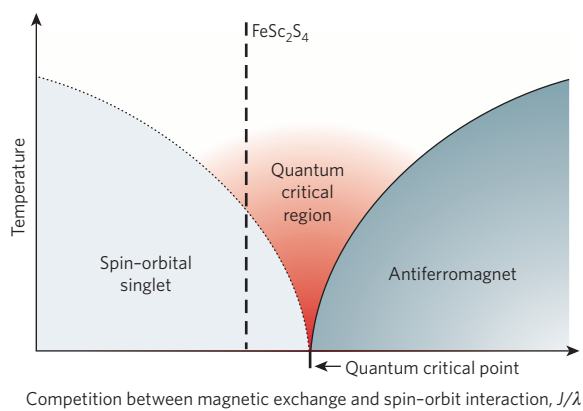


**Figure 5 | Spin-orbital quantum criticality.** Schematic phase diagram of  $\text{FeSc}_2\text{S}_4$ , representing the competition between spin-orbit interaction,  $\lambda$ , and magnetic exchange energy,  $J$ . For large values of  $J/\lambda$ , the spins magnetically order into an antiferromagnetic state. For small  $J/\lambda$ , the spins and orbitals combine into a non-magnetic spin-orbital singlet state. The two ground states are separated by a quantum critical point, which governs the quantum critical region (in the 'fan' above it) at  $T > 0$ . The dashed line indicates the value of  $J/\lambda$  for  $\text{FeSc}_2\text{S}_4$ , which has a large correlation length and small gap as a consequence of its proximity to the quantum critical point.

$S = \frac{1}{2}$ , researchers seem finally to have uncovered QSL ground states, which have long eluded them, but the detailed structures of these have not yet been elucidated. Explaining them will be a theoretical and experimental challenge. In addition, in the process of searching for QSLs, examples of dimensional reduction and quantum criticality were unexpectedly found.

#### Beyond spin ice

The recent observation of magnetic monopoles, in agreement with theory, suggests that there is a good understanding of the interactions and dynamics of the canonical spin-ice materials. The challenge is now to improve this understanding by making a more detailed and accurate comparison of theory and experiment and perhaps by 'engineering' new phenomena through the control of magnetic monopoles. For instance, it might be possible to make spectral measurements of magnetic monopoles by exciting them with neutrons. Some theoreticians have suggested another consequence of emergent electromagnetism in spin ice. If the material can be driven through certain types of phase transition, then exotic critical behaviour in violation of the standard Landau–Ginzburg–Wilson paradigm might be observed<sup>85–87</sup>.

Spin ice certainly proves that there is more to be learned about classical spin liquids, and that these materials are much simpler to understand than their quantum counterparts. In fact, many other materials have classical spin-liquid regimes, and perhaps the ideas that have arisen from studies of spin ice will inspire an understanding of their dynamics. Well-known classical spin liquids include gadolinium gallium garnet and  $\text{SrCr}_{9-x}\text{Ga}_{3+x}\text{O}_{19}$ , both of which have large, predominantly classical spins with very large frustration parameters<sup>80</sup>. Another set of examples is the spinel chromites,  $\text{ACr}_2\text{O}_4$  (where  $\text{A} = \text{Zn, Cd or Hg}$ ), which form  $S = \frac{3}{2}$  Heisenberg pyrochlore antiferromagnets and show a spin-liquid regime with unusual 'loop' structures seen in diffuse neutron scattering<sup>88</sup>. More recently, the A-site spinels  $\text{MnSc}_2\text{S}_4$  (ref. 83) and  $\text{CoAl}_2\text{O}_4$  (ref. 89) have been interpreted in terms of a 'spiral spin liquid'<sup>90</sup>.

Another way to move 'beyond' spin ice is to introduce quantum mechanics. Quantum effects are seen in  $\text{Tb}_2\text{Ti}_2\text{O}_7$ , which in a magnetic field shows many of the anisotropies that are characteristic of spin ice. It avoids freezing or ordering down to  $T = 50$  mK and remains an intriguing theoretical puzzle<sup>6,91</sup>. The material  $\text{Pr}_2\text{Ir}_2\text{O}_7$  combines features of spin ice with metallic conduction<sup>92</sup> and has a zero-field anomalous Hall effect that is indicative of a 'chiral spin liquid' phase.

#### The smoking gun for QSLs

The diversity of QSL candidates and the progress being made towards their theoretical description are encouraging, but the research community is still in the unsatisfactory situation in which the evidence for QSL states is circumstantial and heavily depends on theoretical interpretation. For spin ice, by contrast, there is increasingly direct experimental evidence that magnetic monopoles exist. For QSLs, so far, such a 'smoking gun' is lacking. A conventional experimental technique that could be a candidate for identifying QSLs is inelastic neutron scattering, which the experiments on  $\text{Cs}_2\text{CuCl}_4$  clearly show can reveal spinons under appropriate conditions<sup>69</sup>. This is an important avenue for future experiments, but it would be advantageous to design new experiments specifically to identify QSLs. Some proposals have been made. It has been suggested that a particular class of QSL could display a vortex memory effect, which would probe the existence of the 'vison' excitation of such a spin liquid<sup>93</sup>, but it is extremely difficult to measure this effect in most materials<sup>94</sup>. For QSLs with a spinon Fermi surface or Fermi points, it might be possible to measure ' $2k_F$ ' oscillations, which would be considerable if observed in an insulator. Such observations could be made in neutron-scattering measurements, or they could be made in real space by way of analogues of Friedel oscillation measurements, by using local probes or composite structures<sup>95</sup>.

#### Connections

The physics of frustrated magnetism and spin liquids has intriguing connections to diverse exotic phenomena, many of which are discussed in other articles in this Insight. For example, the modern interest in spin liquids grew largely from Anderson's proposed connection between RVB states and high-temperature copper-oxide-based superconductivity<sup>4</sup>. The idea is that, in an RVB state, electrons bound into valence bonds are paired even though the state is non-superconducting. Thus, part of the physics of superconductivity has already been achieved in this state, and if the material can be made conducting and phase coherent, for example by doping with mobile charges, it will naturally become superconducting. Despite the elegance of this suggestion and decades of theoretical work, RVB superconductivity remains unproven in experiments, although the idea is still actively discussed<sup>96</sup>.

More generally, the problem of frustration and spin-liquid physics in systems with mobile charges is relatively unstudied. There are several interesting materials in which this type of physics can be explored experimentally. I have discussed materials in which such physics might be involved, including the triangular-lattice organic compounds,  $\text{Na}_4\text{Ir}_3\text{O}_8$  and  $\text{Pr}_2\text{Ir}_2\text{O}_7$  (a type of metallic spin ice). Another interesting material in this context is  $2\text{H}-\text{AgNiO}_2$ , a semi-metallic material that shows charge ordering on a triangular lattice<sup>97</sup>. It has been suggested that a novel, continuous Mott transition — rather than the usual discontinuous one — might be observed in such a situation<sup>98,99</sup>.

From the above discussion, it is clear that spin-orbit coupling seems to have an important role in frustrated systems and QSLs. Even in the organic compounds, in which spin-orbit effects are expected to be minimized by the extended molecular orbital states, spin-orbit effects are not obviously negligible. Experiments on  $\kappa-(\text{BEDT-TTF})_2\text{Cu}[\text{N}(\text{CN})_2]\text{Cl}$ , which is a magnetically ordered organic compound, demonstrated a Dzyaloshinskii–Moriya (DM) coupling,  $D$ , of order  $D/k_B \approx 5$  K (ref. 100). If  $\kappa-(\text{BEDT-TTF})_2\text{Cu}[\text{N}(\text{CN})_2]\text{Cl}$  had a similar magnitude of DM coupling it would probably affect many of the low-temperature measurements, such as specific heat and thermal conductivity. In the inorganic materials, DM interactions and other spin-orbit effects are clearly significant and are even dominant in the case of  $\text{Na}_4\text{Ir}_3\text{O}_8$ .

For such materials with strong spin-orbit coupling, it will be interesting to explore the connection to topological insulators (see page 194), which are known to occur in situations with strong spin-orbit coupling and weak correlation. How does the topological insulator evolve with increasing electron localization by Coulomb interactions? Ultimately, with very large values of  $U$ , the strong Mott insulating limit is reached and the system is described by a Heisenberg model, as I have discussed here. It is also interesting to ask how far the physics of topological insula-

tors survives in this direction and whether anything qualitatively new emerges in the presence of both spin-orbit and electronic correlations. The combination of proximity to the Mott transition and strong spin-orbit effects may be common in the late 5d transition metal oxides. A preliminary theoretical study suggests that the physics in this regime could be particularly interesting<sup>101</sup>.

I have only hinted at the abundance of exotic properties of frustrated magnets. Nature has many surprises in store for researchers of these complex materials. It is safe to assume that the exploration of spin liquids will reveal more unexpected phenomena, which might be as interesting as the original objects of the search. ■

1. Ramirez, A. P., Broholm, C. L., Cava, R. J. & Kowach, G. R. Geometrical frustration, spin ice and negative thermal expansion — the physics of underconstraint. *Physica B* **280**, 290–295 (2000).
2. Kléman, M., Lavrentovich, O. D. & Friedel, J. *Soft Matter Physics: An Introduction* (Springer, 2003).
3. Wannier, G. H. Antiferromagnetism. The triangular Ising net. *Phys. Rev.* **79**, 357–364 (1950).
4. Anderson, P. W. The resonating valence bond state in  $\text{La}_2\text{CuO}_4$  and superconductivity. *Science* **235**, 1196–1198 (1987).
5. Bramwell, S. T. & Gingras, M. J. P. Spin ice state in frustrated magnetic pyrochlore materials. *Science* **294**, 1495–1501 (2001).
- This is an excellent review of the physics of spin ice that was published before the recent work on Coulomb correlations and monopoles.
6. Gingras, M. J. P. in *Highly Frustrated Magnetism* (eds Lacroix, C., Mendels, P. & Mila, F.) (Springer, in the press); preprint at (<http://arXiv.org/abs/0903.2772>) (2009).
7. Harris, M. J., Bramwell, S. T., McMorrow, D. F., Zeiske, T. & Godfrey, K. W. Geometrical frustration in the ferromagnetic pyrochlore  $\text{Ho}_2\text{Ti}_2\text{O}_7$ . *Phys. Rev. Lett.* **79**, 2554–2557 (1997).
8. Isakov, S. V., Moessner, R. & Sondhi, S. L. Why spin ice obeys the ice rules. *Phys. Rev. Lett.* **95**, 217201 (2005).
9. den Hertog, B. C. & Gingras, M. J. P. Dipolar interactions and origin of spin ice in Ising pyrochlore magnets. *Phys. Rev. Lett.* **84**, 3430–3433 (2000).
10. Ramirez, A. P., Hayashi, A., Cava, R. J., Siddharthan, R. & Shastry, B. S. Zero-point entropy in 'spin ice'. *Nature* **399**, 333–334 (1999).
11. Pauling, L. The structure and entropy of ice and of other crystals with some randomness of atomic arrangement. *J. Am. Chem. Soc.* **57**, 2680–2684 (1935).
12. Youngblood, R., Axe, J. D. & McCoy, B. M. Correlations in ice-rule ferroelectrics. *Phys. Rev. B* **21**, 5212–5220 (1980).
13. Isakov, S. V., Gregor, K., Moessner, R. & Sondhi, S. L. Dipolar spin correlations in classical pyrochlore magnets. *Phys. Rev. Lett.* **93**, 167204 (2004).
14. Henley, C. L. Power-law spin correlations in pyrochlore antiferromagnets. *Phys. Rev. B* **71**, 014424 (2005).
15. Fennell, T. et al. Experimental proof of a magnetic Coulomb phase. Preprint at (<http://arXiv.org/abs/0907.0954>) (2009).
16. Castelnovo, C., Moessner, R. & Sondhi, S. L. Magnetic monopoles in spin ice. *Nature* **451**, 42–45 (2008).
- This theoretical paper proposed that magnetic monopoles are present in spin ice.
17. Jaubert, L. D. C. & Holdsworth, P. C. W. Signature of magnetic monopole and Dirac string dynamics in spin ice. *Nature Phys.* **5**, 258–261 (2009).
- This paper shows how the density and dynamics of magnetic monopoles can be inferred from the experimental magnetization relaxation rate in spin ice.
18. Onsager, L. Deviations from Ohm's law in weak electrolytes. *J. Chem. Phys.* **2**, 599–615 (1934).
19. Bramwell, S. T. et al. Measurement of the charge and current of magnetic monopoles in spin ice. *Nature* **461**, 956–959 (2009).
- This paper extracts an experimental value for the charge of a magnetic monopole in spin ice, on the basis of an analogy of the monopole plasma to a classical electrolyte.
20. Morris, D. J. P. et al. Dirac strings and magnetic monopoles in the spin ice  $\text{Dy}_2\text{Ti}_2\text{O}_7$ . *Science* **326**, 411–414 (2009).
21. Kadokawa, H. et al. Observation of magnetic monopoles in spin ice. *J. Phys. Soc. Jpn* **78**, 103706 (2009).
22. Anderson, P. W. Resonating valence bonds: a new kind of insulator. *Mater. Res. Bull.* **8**, 153–160 (1973).
- This paper proposed the RVB wavefunction for a QSL state.
23. Iwase, H., Isobe, M., Ueda, Y. & Yasuoka, H. Observation of spin gap in  $\text{CaV}_2\text{O}_5$  by NMR. *J. Phys. Soc. Jpn* **65**, 2397–2400 (1996).
24. Azuma, M., Hiroi, Z., Takano, M., Ishida, K. & Kitaoka, Y. Observation of a spin gap in  $\text{SrCu}_2\text{O}_3$  comprising spin-½ quasi-1D two-leg ladders. *Phys. Rev. Lett.* **73**, 3463–3466 (1994).
25. Kageyama, H. et al. Exact dimer ground state and quantized magnetization plateaus in the two-dimensional spin system  $\text{SrCu}_2(\text{BO}_3)_2$ . *Phys. Rev. Lett.* **82**, 3168–3171 (1999).
26. Nikuni, T., Oshikawa, M., Oosawa, A. & Tanaka, H. Bose-Einstein condensation of dilute magnons in  $\text{TiCuCl}_3$ . *Phys. Rev. Lett.* **84**, 5868–5871 (2000).
27. Moessner, R. & Sondhi, S. L. Resonating valence bond phase in the triangular lattice quantum dimer model. *Phys. Rev. Lett.* **86**, 1881–1884 (2001).
28. Kitaev, A. Anyons in an exactly solved model and beyond. *Ann. Phys. (Leipzig)* **321**, 2–111 (2006).
29. Motrunich, O. I. & Senthil, T. Exotic order in simple models of bosonic systems. *Phys. Rev. Lett.* **89**, 277004 (2002).
30. Balents, L., Fisher, M. P. A. & Girvin, S. M. Fractionalization in an easy-axis kagomé antiferromagnet. *Phys. Rev. B* **65**, 224412 (2002).
31. Hermele, M., Fisher, M. P. A. & Balents, L. Pyrochlore photons: the U(1) spin liquid in a  $S = \frac{1}{2}$  three-dimensional frustrated magnet. *Phys. Rev. B* **69**, 064404 (2004).
32. Levin, M. A. & Wen, X. G. String-net condensation: a physical mechanism for topological phases. *Phys. Rev. B* **71**, 045110 (2005).
33. Liang, S., Doucot, B. & Anderson, P. W. Some new variational resonating-valence-bond-type wave functions for the spin-½ antiferromagnetic Heisenberg model on a square lattice. *Phys. Rev. Lett.* **61**, 365–368 (1988).
34. Alet, F., Walczak, A. M. & Fisher, M. P. A. Exotic quantum phases and phase transitions in correlated matter. *Physica A* **369**, 122–142 (2006).
35. Wen, X. G. Quantum orders and symmetric spin liquids. *Phys. Rev. B* **65**, 165113 (2002).
36. Read, N. & Sachdev, S. Large- $N$  expansion for frustrated quantum antiferromagnets. *Phys. Rev. Lett.* **66**, 1773–1776 (1991).
37. Affleck, I. & Marston, J. B. Large- $n$  limit of the Heisenberg-Hubbard model: implications for high- $T_c$  superconductors. *Phys. Rev. B* **37**, 3774–3777 (1988).
38. Rantner, W. & Wen, X.-G. Electron spectral function and algebraic spin liquid for the normal state of underdoped high  $T_c$  superconductors. *Phys. Rev. Lett.* **86**, 3871–3874 (2001).
39. Lee, P. A. An end to the drought of quantum spin liquids. *Science* **321**, 1306–1307 (2008).
40. Ramirez, A. P. Quantum spin liquids: a flood or a trickle? *Nature Phys.* **4**, 442–443 (2008).
41. Olariu, A. et al.  $^{17}\text{O}$  NMR study of the intrinsic magnetic susceptibility and spin dynamics of the quantum kagomé antiferromagnet  $\text{ZnCu}_3(\text{OH})_6\text{Cl}_2$ . *Phys. Rev. Lett.* **100**, 087202 (2008).
42. Yoshida, H. et al. Magnetization 'steps' on a kagomé lattice in volborthite. *J. Phys. Soc. Jpn* **78**, 043704 (2009).
43. Kuroasaki, Y., Shimizu, Y., Miyagawa, K., Kanoda, K. & Saito, G. Mott transition from a spin liquid to a Fermi liquid in the spin-frustrated organic conductor  $\kappa$ -(ET)<sub>2</sub>Cu<sub>2</sub>(CN)<sub>3</sub>. *Phys. Rev. Lett.* **95**, 177001 (2005).
44. Shimizu, Y., Akimoto, H., Tsuji, H., Tajima, A. & Kato, R. Mott transition in a valence-bond solid insulator with a triangular lattice. *Phys. Rev. Lett.* **99**, 256403 (2007).
45. Kézsmárki, I. et al. Depressed charge gap in the triangular-lattice Mott insulator  $\kappa$ -(ET)<sub>2</sub>Cu<sub>2</sub>(CN)<sub>3</sub>. *Phys. Rev. B* **74**, 201101 (2006).
46. Okamoto, Y., Nohara, M., Aruga-Katori, H. & Takagi, H. Spin-liquid state in the  $S = \frac{1}{2}$  hyperkagomé antiferromagnet  $\text{Na}_4\text{Ir}_3\text{O}_8$ . *Phys. Rev. Lett.* **99**, 137207 (2007).
47. Okamoto, Y., Yoshida, H. & Hiroi, Z. Vesignieite  $\text{BaCu}_3\text{V}_2\text{O}_8(\text{OH})_2$  as a candidate spin-½ kagomé antiferromagnet. *J. Phys. Soc. Jpn* **78**, 033701 (2009).
48. Hiroi, Z. et al. Spin-½ kagomé-like lattice in volborthite,  $\text{Cu}_3\text{V}_2\text{O}_7(\text{OH})_2\text{H}_2\text{O}$ . *J. Phys. Soc. Jpn* **70**, 3377–3384 (2001).
49. Helton, J. S. et al. Spin dynamics of the spin-½ kagomé lattice antiferromagnet  $\text{ZnCu}_3(\text{OH})_6\text{Cl}_2$ . *Phys. Rev. Lett.* **98**, 107204 (2007).
50. Ramirez, A. P. Strongly geometrically frustrated magnets. *Annu. Rev. Mater. Sci.* **24**, 453–480 (1994).
- This review helped to define the field of highly frustrated magnets and is an excellent discussion of the state of the science at the time.
51. Yamashita, S. et al. Thermodynamic properties of a spin-½ spin-liquid state in a  $\kappa$ -type organic salt. *Nature Phys.* **4**, 459–462 (2008).
52. Shimizu, Y., Miyagawa, K., Kanoda, K., Maesato, M. & Saito, G. Spin liquid state in an organic Mott insulator with a triangular lattice. *Phys. Rev. Lett.* **91**, 107001 (2003).
53. Itoh, T., Oyamada, A., Maegawa, S., Tamura, M. & Kato, R. Quantum spin liquid in the spin-½ triangular antiferromagnet  $\text{EtMe}_3\text{Sb}[\text{Pd}(\text{dmit})_2]$ . *Phys. Rev. B* **77**, 104413 (2008).
54. Itoh, T., Oyamada, A., Maegawa, S., Tamura, M. & Kato, R. Spin-liquid state in an organic spin-½ system on a triangular lattice,  $\text{EtMe}_3\text{Sb}[\text{Pd}(\text{dmit})_2]$ . *J. Phys. Condens. Matter* **19**, 145247 (2007).
55. Mendels, P. et al. Quantum magnetism in the paratacamite family: towards an ideal kagomé lattice. *Phys. Rev. Lett.* **98**, 077204 (2007).
56. Yoshida, M., Takigawa, M., Yoshida, H., Okamoto, Y. & Hiroi, Z. Phase diagram and spin dynamics in volborthite with a distorted kagomé lattice. *Phys. Rev. Lett.* **103**, 077207 (2009).
57. Koretsune, T., Motome, Y. & Furusaki, A. Exact diagonalization study of Mott transition in the Hubbard model on an anisotropic triangular lattice. *J. Phys. Soc. Jpn* **76**, 074719 (2007).
58. Kyung, B. & Tremblay, A. M. S. Mott transition, antiferromagnetism, and d-wave superconductivity in two-dimensional organic conductors. *Phys. Rev. Lett.* **97**, 046402 (2006).
59. Morita, H., Watanabe, S. & Imada, M. Nonmagnetic insulating states near the Mott transitions on lattices with geometrical frustration and implications for  $\kappa$ -(ET)<sub>2</sub>Cu<sub>2</sub>(CN)<sub>3</sub>. *J. Phys. Soc. Jpn* **71**, 2109–2112 (2002).
60. Lecheminant, P., Bernu, B., Lhuillier, C., Pierre, L. & Sindzingre, P. Order versus disorder in the quantum Heisenberg antiferromagnet on the kagomé lattice using exact spectra analysis. *Phys. Rev. B* **56**, 2521–2529 (1997).
61. Marston, J. B. & Zeng, C. Spin-Peierls and spin-liquid phases of kagomé quantum antiferromagnets. *J. Appl. Phys.* **69**, 5962 (1991).
62. Singh, R. R. P. & Huse, D. A. Ground state of the spin-½ kagomé lattice Heisenberg antiferromagnet. *Phys. Rev. B* **76**, 180407 (2007).
63. Cépas, O., Fong, C. M., Leung, P. W. & Lhuillier, C. Quantum phase transition induced by Dzyaloshinskii-Moriya interactions in the kagomé antiferromagnet. *Phys. Rev. B* **78**, 140405 (2008).
64. Chen, G. & Balents, L. Spin-orbit effects in  $\text{Na}_4\text{Ir}_3\text{O}_8$ : a hyperkagomé lattice antiferromagnet. *Phys. Rev. B* **78**, 094403 (2008).
65. Motrunich, O. I. Variational study of triangular lattice spin-½ model with ring exchanges and spin liquid state in  $\kappa$ -(ET)<sub>2</sub>Cu<sub>2</sub>(CN)<sub>3</sub>. *Phys. Rev. B* **72**, 045105 (2005).
66. Lee, S.-S. & Lee, P. A. U(1) gauge theory of the Hubbard model: spin liquid states and possible application to  $\kappa$ -(BEDT-TTF)<sub>2</sub>Cu<sub>2</sub>(CN)<sub>3</sub>. *Phys. Rev. Lett.* **95**, 036403 (2005).
67. Ran, Y., Hermele, M., Lee, P. A. & Wen, X. G. Projected-wave-function study of the spin-½ Heisenberg model on the kagomé lattice. *Phys. Rev. Lett.* **98**, 117205 (2007).
68. Lawler, M. J., Paramesaki, A., Kim, Y. B. & Balents, L. Gapless spin liquids on the three-dimensional hyperkagomé lattice of  $\text{Na}_4\text{Ir}_3\text{O}_8$ . *Phys. Rev. Lett.* **101**, 197202 (2008).
69. Coldea, R., Tennant, D. A. & Tytlczynski, Z. Extended scattering continua characteristic of spin fractionalization in the two-dimensional frustrated quantum magnet  $\text{Cs}_2\text{CuCl}_4$  observed by neutron scattering. *Phys. Rev. B* **68**, 134424 (2003).
70. Coldea, R., Tennant, D. A., Tsvelik, A. M. & Tytlczynski, Z. Experimental realization of a 2D fractional quantum spin liquid. *Phys. Rev. Lett.* **86**, 1335–1338 (2001).

71. Lake, B., Tennant, D. A., Frost, C. D. & Nagler, S. E. Quantum criticality and universal scaling of a quantum antiferromagnet. *Nature Mater.* **4**, 329–334 (2005).

72. Bocquet, M., Essler, F. H. L., Tsvelik, A. M. & Gogolin, A. O. Finite-temperature dynamical magnetic susceptibility of quasi-one-dimensional frustrated spin-½ Heisenberg antiferromagnets. *Phys. Rev. B* **64**, 094425 (2001).

73. Starykh, O. A. & Balents, L. Ordering in spatially anisotropic triangular antiferromagnets. *Phys. Rev. Lett.* **98**, 077205 (2007).

74. Kohno, M., Starykh, O. A. & Balents, L. Spinons and triplons in spatially anisotropic frustrated antiferromagnets. *Nature Phys.* **3**, 790–795 (2007).  
This theoretical paper shows how a model of interacting 1D spinons can quantitatively explain inelastic neutron scattering in  $\text{Cs}_2\text{CuCl}_4$ .

75. Fortune, N. A. *et al.* Cascade of magnetic-field-induced quantum phase transitions in a spin-½ triangular-lattice antiferromagnet. *Phys. Rev. Lett.* **102**, 257201 (2009).

76. Khomskii, D. I. Role of orbitals in the physics of correlated electron systems. *Phys. Scr.* **72**, CC8–CC14 (2005).

77. Tokura, Y. & Nagaosa, N. Orbital physics in transition-metal oxides. *Science* **288**, 462–468 (2000).

78. Ishihara, S., Yamanaka, M. & Nagaosa, N. Orbital liquid in perovskite transition-metal oxides. *Phys. Rev. B* **56**, 686–692 (1997).

79. Feiner, L. F., Olés, A. M. & Zaanen, J. Quantum melting of magnetic order due to orbital fluctuations. *Phys. Rev. Lett.* **78**, 2799–2802 (1997).

80. Khaliullin, G. & Maekawa, S. Orbital liquid in three-dimensional Mott insulator:  $\text{LaTiO}_3$ . *Phys. Rev. Lett.* **85**, 3950–3953 (2000).

81. Büttgen, N., Zymara, A., Kegler, C., Tsurkan, V. & Loidl, A. Spin and orbital frustration in  $\text{FeSc}_2\text{S}_4$  probed by  $^{45}\text{Sc}$  NMR. *Phys. Rev. B* **73**, 132409 (2006).

82. Krimmel, A. *et al.* Vibronic and magnetic excitations in the spin-orbital liquid state of  $\text{FeSc}_2\text{S}_4$ . *Phys. Rev. Lett.* **94**, 237402 (2005).

83. Fritsch, V. *et al.* Spin and orbital frustration in  $\text{MnSc}_2\text{S}_4$  and  $\text{FeSc}_2\text{S}_4$ . *Phys. Rev. Lett.* **92**, 116401 (2004).

84. Chen, G., Balents, L. & Schnyder, A. P. A. Spin-orbital singlet and quantum critical point on the diamond lattice:  $\text{FeSc}_2\text{S}_4$ . *Phys. Rev. Lett.* **102**, 096406 (2009).

85. Powell, S. & Chalker, J. T. Classical to quantum mappings for geometrically frustrated systems: spin-ice in a [100] field. *Phys. Rev. B* **78**, 024422 (2008).

86. Saunders, T. E. & Chalker, J. T. Structural phase transitions in geometrically frustrated antiferromagnets. *Phys. Rev. B* **77**, 214438 (2008).

87. Bergman, D. L., Fiete, G. A. & Balents, L. Ordering in a frustrated pyrochlore antiferromagnet proximate to a spin liquid. *Phys. Rev. B* **73**, 134402 (2006).

88. Lee, S. H. *et al.* Emergent excitations in a geometrically frustrated magnet. *Nature* **418**, 856–858 (2002).

89. Tristan, N. *et al.* Geometric frustration in the cubic spinels  $\text{MAl}_2\text{O}_4$  (M = Co, Fe, and Mn). *Phys. Rev. B* **72**, 174404 (2005).

90. Bergman, D., Alicea, J., Gull, E., Trebst, S. & Balents, L. Order by disorder and spiral spin liquid in frustrated diamond lattice antiferromagnets. *Nature Phys.* **3**, 487–491 (2007).

91. Gardner, J. S. *et al.* Cooperative paramagnetism in the geometrically frustrated pyrochlore antiferromagnet  $\text{Tb}_2\text{Ti}_2\text{O}_7$ . *Phys. Rev. Lett.* **82**, 1012–1015 (1999).

92. Nakatsuji, S. *et al.* Metallic spin-liquid behavior of the geometrically frustrated Kondo lattice. *Phys. Rev. Lett.* **96**, 087204 (2006).

93. Senthil, T. & Fisher, M. P. A. Fractionalization in the cuprates: detecting the topological order. *Phys. Rev. Lett.* **86**, 292–295 (2001).

94. Wynn, J. C. *et al.* Limits on spin-charge separation from  $h/2e$  fluxoids in very underdoped  $\text{YBa}_2\text{Cu}_6\text{O}_{6+\delta}$ . *Phys. Rev. Lett.* **87**, 197002 (2001).

95. Norman, M. R. & Micklitz, T. How to measure a spinon Fermi surface. *Phys. Rev. Lett.* **102**, 067204 (2009).

96. Lee, P. A., Nagaosa, N. & Wen, X. G. Doping a Mott insulator: physics of high-temperature superconductivity. *Rev. Mod. Phys.* **78**, 17–85 (2006).  
The main subject of this paper is superconductivity, but it provides a good summary of the status of the theory of QSL states.

97. Wawrzynska, E. *et al.* Orbital degeneracy removed by charge order in triangular antiferromagnet  $\text{AgNiO}_2$ . *Phys. Rev. Lett.* **99**, 157204 (2007).

98. Podolsky, D., Parameswari, A., Kim, Y. B. & Senthil, T. Mott transition between a spin-liquid insulator and a metal in three dimensions. *Phys. Rev. Lett.* **102**, 186401 (2009).

99. Senthil, T. Theory of a continuous Mott transition in two dimensions. *Phys. Rev. B* **78**, 045109 (2008).

100. Smith, D. F. *et al.* Dzialoshinskii–Moriya interaction in the organic superconductor  $\kappa$ -(BEDT-TTF)<sub>2</sub>Cu[N(CN)<sub>2</sub>]Cl. *Phys. Rev. B* **68**, 024512 (2003).

101. Pesin, D. A. & Balents, L. Mott physics and band topology in materials with strong spin-orbit interaction. Preprint at (<http://arxiv.org/abs/0907.2962>) (2009).

**Acknowledgements** I am grateful to countless friends and collaborators, especially O. Starykh and M. Fisher for many stimulating interactions. I would also like to thank R. Coldea, H. Takagi, A. Loidl and P. Mendels for sharing their insights into experiments on frustrated magnets. My research is supported by the US National Science Foundation, the US Department of Energy, the David and Lucile Packard Foundation and the US Army Research Office.

**Author Information** Reprints and permissions information is available at [www.nature.com/reprints](http://www.nature.com/reprints). The author declares no competing financial interests. Correspondence should be addressed to the author (balents@kitp.ucsb.edu).